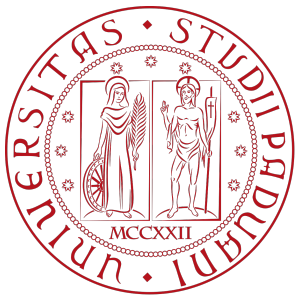

UNIVERSITÀ DEGLI STUDI DI PADOVA

Dipartimento di Fisica e Astronomia "Galileo Galilei"

Corso di Laurea in Fisica

Tesi di Laurea Triennale

Virus inactivation through cold plasma application: a review

Relatore

Prof. Emilio Martines

Laureando

Cristina Venturini

Anno Accademico 2019/2020

Abstract

One of the main objects of research in the field of the application of ionized gases (plasmas) for therapeutic purposes (plasma medicine) is that of disinfection, mainly obtained by chemical reactive oxygen and nitrogen species, formed by the action of a low temperature plasma. The majority of studies on this subject cover the action of plasma on bacteria and, in a lesser measure, fungi. In the wake of the Covid-19 epidemic, it is of great interest to study the possibilities offered by this technology for what concerns virus inactivation.
The purpose of this thesis is to draw up a review of the existent literature on the effect of low temperature plasmas on viruses, dividing the consulted articles on the basis of the technology used to generate the plasma and the resulting physical parameters.

Contents

Abbreviations

The following abbreviations will be used:

DBD	Dielectric Barrier Discharge	**EEDF**	Electron Energy Distribution Function
RF	Radio Frequency	**RONS**	Reactive Oxygen Nitrogen Species
APPJ	Atmospheric Pressure Plasma Jet	**ROS**	Reactive Oxygen Species
APP	Atmospheric Pressure Plasma	**RON**	Reactive Nitrogen Species
CAP	Cold Atmospheric Plasma	**APGD**	Atmospheric Pressure Glow Discharge
CP	Cold Plasma	**SMD**	Surface Micro Discharge
APCP	Atmospheric Pressure Cold Plasma	**HV**	High Voltage
PAS	Plasma Activated Solution	**CAPP**	Cold Atmospheric Pressure Plasma
PAW	Plasma Activated Water	**HEDBS**	Hollow Electrodes Dielectric Barrier Structure

Introduction

The term plasma refers to the fourth state of matter, in which part of the gas molecules are ionized, meaning that they are split into ions and electrons. This state lends peculiar characteristics to the matter, such as making it highly electrically conductive and granting it a high sensitivity to external magnetic fields.
It is important to remark that despite the ionization and sensitivity to electro-magnetic fields, the gas is still globally neutral.
Most of the matter in the universe lies in the state of plasma (stars, intracluster medium) but on earth it can be found only in peculiar circumstances, like flames or lightning, or it can be created in laboratories, in different ways and sizes (from large experiments to miniaturized plasma sources). The remarkable properties of plasma have been known for many decades and humanity has studied them for many applications: clean energy production (nuclear fusion), industrial applications (etching, deposition of thin films, plasma furnaces amongst others), space travel (plasma propulsion engine) and medicine. In all these fields plasmas are used in different ways and especially under different conditions; in fact, plasmas are generally divided into thermal plasmas, where all the components (ions, electrons and neutral particles) reach a high temperature, and non-thermal plasmas, also called low-temperature or cold plasmas, where only the electrons are heated to a high temperature. Depending on the field of application, cold or thermal plasmas can be used, for example in nuclear fusion the use of the latter is necessary, while for certain uses of plasma medicine it is mandatory for the plasma to be non-thermal. Plasmas can also be classified by their degree of ionization: most plasmas are weakly ionized, meaning that only a small fraction of the molecules is ionized. This is the case, for example, of cold plasmas at atmospheric pressure, while fusion plasmas, which are way hotter, are totally ionized.
Although the plasma state was first described in the 1920s by Irvin Langmuir, the discipline of plasma medicine began to appear only more recently, in the last 20 years. During this time, several studies have demonstrated the beneficial properties of plasmas, both on inanimate surfaces and living tissues, leading the way to an ever-growing field of applied physics. Plasma medicine applications use different type of plasmas, both thermal (surgical scalpels, sterilization of inanimate objects) and non-thermal. While the thermal applications have been around for quite some years, the low temperature ones have started to gain momentum only more recently; it is worth mentioning that non-thermal plasmas used in the medical field are also atmospheric pressure plasmas and are generally called CAP. In fact, usually plasmas are produced ionizing a low-pressure gas, because this kind of condition eases the ionization of atoms, but for medical purposes it is important to be able to use the plasma device at atmospheric pressures.
Some of the uses of CAPs include plasma-based treatment of chronic wounds, dental cavities treatment, tissue engineering, treatment of skin diseases [1] and eye diseases [2] and tumour treatment based on the possibility to selectively trigger the apoptosis (programmed cell death) of cancer cells. In particular, the ability of CAPs to disinfect both inanimate objects or surfaces and living tissues has been widely studied for what concerns fungi and bacteria and in a lesser measure for viruses.
This kind of studies acquire an even greater importance if we consider the situation we are living right now: the COVID-19 pandemic has already severely damaged a vast majority of countries and especially in Italy the toll taken on the population (and the economy) has been extremely severe. During these times, apart from a vaccine, the most wanted thing is effective disinfection of surfaces and living tissues (specifically, hands); it can then be understood the relevance acquired by studies on CAP for virus deactivation. Not only devices based on this kind of technology could efficiently disinfect surfaces and living tissues, without unwanted thermal effects, but they would also represent a green

alternative to often poisonous chemical disinfectants [3], also considering the fact that it is possible to produce what is called plasma activated water, which is storable, transportable and maintains the disinfecting properties of the plasma [3].
This work will aim at giving a review of the existent studies on disinfection by CAP, for what concerns viruses, focusing on the plasma source features, characterizing the geometry of the electrodes, the gas used to ignite the plasma, and the kind of voltage used to power the device and generate the plasma.
The thesis will therefore be structured as follows:

- first, some basic concepts on how CAP devices for virus deactivation work will be presented, focusing on the kind of source (DBD, RF, UV), the electrode geometry, the gas mixture and giving some basic outlines on how plasma-virus interaction works, mainly to explain why certain configurations and gas mixtures are preferred;
- an overview of the articles regarding deactivation of virus by CAP will be made, divided in three sections, on the basis of the plasma source: DBD, RF, UV;
- a table will be presented, summarising the main information contained in every article that has here been reviewed (Table 3.1);
- conclusions will be drawn.

Chapter 1

General properties of CAP devices for virus deactivation

CAPs used for virus deactivation can be divided in two categories, depending on the way the plasma is generated: DBD (dielectric barrier discharge) or RF (radio frequency). A study that uses an UV kind of source was also considered, but represented a single case amongst the consulted literature.

1.1 Plasma source: DBD

Theodose du Moncel was the first to realize that it was possible to induce a plasma between two conducting plates separated by a dielectric medium (1853); after him few other early works were carried out, by Werner von Siemens in 1857 and by Von Engel in the 1930s but further investigations on the subject have been resumed only much later, around the late 1980s and the early 1990s, when the generation of relatively large volume, nonequilibrium, diffuse atmospheric pressure plasma by the Dielectric Barrier Discharge (DBD) technique was successfully carried out as reported by Kanazawa et al [4], Massines et al [5], and Roth et al [6]. These authors mostly used a planar geometry and sinusoidal voltages in kV at frequencies in the order of 10 kHz. To improve the performance of the DBD, fast rise time voltage pulses with pulse widths in the nanoseconds-microseconds range were employed; the advantage of these pulses was that they made it possible to preferentially couple the applied energy to the electrons and to control the electron energy distribution function (EEDF) which allows to enhance the plasma chemistry responsible for the biological effects. [7]
In fact, the electron energy distribution basically single-handedly defines the plasma chemistry: through electron impact excitation radicals and RONS are produced. By using pulses with a width less than the characteristic time of the onset of the glow-to-arc transition it is possible to increase ionization and to reach higher values for the electron energy distribution and also keep the plasma more stable. In DBDs, at least one of the electrodes is covered in dielectric material, with the most common ones being glass, quartz, ceramics, and polymers. The distance between the electrodes can vary considerably, ranging from less than 0.1 mm in plasma screens, to several millimetres in ozone generators and to several centimetres in CO_2 lasers. There are several different configurations, but the most common ones are planar, which uses parallel plates separated by a dielectric, cylindrical or coaxial plates with a dielectric tube between them. DBDs can be generated in a volume, and they are then called V-DBD, or on a surface, called S-DBD; for volumetric ones the plasma is generated between two electrodes, for example parallel plates with one or two dielectrics amongst them, while for S-DBD the plasma is generated on the surface of the dielectric and so the discharges are limited to the surface. As said before, high sinusoidal voltages in the kV range with frequency in the kHz range energize the electrodes. The electrodes arrangement is usually contained in a vessel to allow the flow of the gas mixture. After having applied voltage, surface charges start to gather on the dielectric surface, and they generate a potential, which counteracts the one associated with the external applied voltage, thus self-limiting the discharge current; this charge accumulation on the surface of the dielectric plays a key role in maintaining the nonequilibrium nature of the plasma. [7]
Initially DBDs could only produce filamentary plasmas, which resulted in non uniform surface treat-

ment, but more recently, starting with Kanazawa et al in the late 1980s, studies showing the possibility of generating a diffuse uniform plasma have been published. Specifically, for Kanazawa et al the necessary operating conditions were using helium as gas and an operating frequency in the range of kHz; other authors managed to generate diffuse plasmas with other gases and at different frequencies. It was Massines et al that proposed the mechanism that leads to a diffuse plasma, identifying seed electrons and metastable atoms available between current pulses as responsible for gas breakdown under low electric field conditions. The seed electrons are electrons that have been left over from the previous current pulse and (or) those produced by Penning ionization. These seed particles can allow a Townsend-type breakdown or a glow discharge, depending on the type of gas used (nitrogen or helium). If helium is used, a density of seed electrons greater than 10^6 cm^{-3} is found to be sufficient to maintain the plasma ignited under low field conditions. If nitrogen is used, the metastable atoms are the ones keeping the discharge ignited between pulses; in this case the surface of the dielectric plays a key role. [7]

1.2 Plasma source: RF

Radio frequency (RF) plasmas are plasmas that have been ignited using a voltage lower than that used to ignite DBDs and frequencies in the MHz range.
To give a brief introduction on these kind of discharges, it is useful to address the differences between RF and DBDs and to distinguish between capacitive and inductive coupling, two different ways of coupling energy to the plasma.

1.2.1 Capacitive coupling

As previously stated, usually in DBDs the external electric energy is coupled into the gas plasma through the electric field established between two electrodes. This kind of energy coupling is called capacitive coupling and the resulting plasma is a capacitive coupled plasma.
Generally speaking the discharge current is composed of two different kinds of current: a conduction current and a displacement current. The first one results from electrical conduction of the electrons from one electrode to the other and it is supplied by the unbound electrons released from an electrical discharge, this means it only exists in the presence of plasma. The second one emerges because of temporal variation of the applied voltage and as such it is always present: as the excitation frequency rises it follows, generally contributing to determine a larger total discharge current, and sometimes a higher electron density, at high frequencies. [8]
The most common cold atmospheric plasmas at high frequency are those sustained at radiofrequencies (RF), namely in the 1-30 MHz range, also called RF atmospheric pressure glow-discharges (APGD), because they tend to be ignited immediately in glow mode. If compared to DBDs at 10-50 kHz, RF plasmas need lower applied voltage and larger discharge current to be sustained, because of low breakdown voltage and high displacement current at high frequencies. To compare and give some numbers, considering a typical DBD in helium at 20 kHz the peak voltage would be 3-7 kV and peak discharge current at 10-200 mA; with the same electrode geometry and structure, a RF plasma at 13.56 MHz (industrially used frequency) will have a peak voltage of approximately a few hundred volts and a peak discharge current of a few amperes. The dissipated electrical power density will be greater by one order of magnitude for the RF than for the DBD. [8]
Electron dynamics in a RF APGD will be significantly different from the DBD one, because of low applied voltages and high frequency. In fact, during one half period of frequency the electric field does not change its polarity; electrons are accelerated by the external low voltage and start moving towards the instantaneous anode, which they can't reach, because the half period is really short at this high frequencies (17-500 ns). Consequentially, the phenomenon of electron trapping happens: most electrons are kept between the two electrodes and their acceleration is maintained by the oscillating RF voltage through many RF periods. This is responsible for sustained ionization and higher electron density. The plasma is therefore sustained continuously, differing from the discrete DBD plasma. This additionally provides an effective mechanism to suppress unlimited growth of the discharge current and as a consequence dielectric barriers are not necessary in RF ignited plasmas.

There are two different operative modes in RF APGD, a low current mode, α mode, and a high current mode, γ mode. To obtain effective plasma chemistry, the γ mode is preferred, but it is also the most susceptible to the glow-to-arc transition and is therefore not always possible to efficiently control it and making it reproduce specific operating conditions. This is one of the cases in which the use of dielectric barriers is necessary even with RF APGD.
By increasing the frequency the difference between DBD and RF APGD becomes clearer and clearer until $\sim$ 50 MHz, behind that point the half period during which electrons can be accelerated without the polarity getting reversed, becomes shorter and shorter (<10 ns) and the maximal kinetic energy reachable by the electrons is reduced. The high frequency range of the spectrum (30-300 MHz) is also called VHF band, here the decrease availability of energetic electrons diminishes the plasma reactivity. [8] Elevated frequency also involves a rise in temperature, because of the higher number of electron collisions with neutral particles; to mitigate this, pulsed RF atmospheric plasmas have been proposed, in which the magnitude of the applied voltage is pulse mitigated. [8]

1.2.2 Inductive coupling

Instead of using a pair of electrodes it is possible to employ one or more electrical wires rolled around a tube and ignite an electrical discharge of a gas passing through the tube. The electric current flowing in the wires generates a time dependent magnetic field, which by means of magnetic induction sets up a time varying electric field which is responsible for the breakdown of the gas. In this way the external energy is inductively coupled to the plasma, since the electric field is generated through magnetic induction and the wire acts as an inductor. Plasma generated in this way are called inductively coupled plasmas. It is worth mentioning that inductively coupled plasmas can be generated also with a planar structure, not only with a cilindrical one.
Low pressure inductively coupled plasmas offer a wide range of advantages, such as high plasma density and separate control of plasma density and ion energy. Such advantages can be exploited even at atmospheric pressure but with a major drawback for what concerns medical applications: higher gas temperature and therefore unwanted thermal effects. To use these plasmas for medical applications, some authors have cooled the inductively produced plasma through its heat exchange with surrounding air; such procedure can lower plasma temperature at the core to at least a couple thousand degrees. [8]
In none of the papers analyzed in this thesis the plasma was produced by inductive coupling.

1.3 Plasma source: UV

In one of the articles reviewed (Chapter 3) a plasma generated by a UV source is mentioned. This kind of source would use an UV radiation source, emitting in a specific wavelength, corresponding to photons with a specific energy which would then proceed to ionize particles of the gas, catalizing the process known as *electron avalanche*. Specifically, remembering that 1 eV corresponds to a frequency of $2.42 \cdot 10^{14}$ Hz and a wavelength of 1240 nm, and the ionization potential is typically in the range 5-25 eV, the electromagnetic radiation capable of producing ionization events is limited to UV radiation, X-rays and gamma rays.

1.4 Plasma-Virus interaction

To understand how the disinfection mechanism works, it is first needed to address the composition of CAPs: ions, free electrons and neutral particles belonging to the main process gas (typically helium, argon, or sometimes directly air), but also reactive species, including atoms (O and N), molecules (O_3, H_2O_2, and HNO_2), radicals ($OH^\bullet$, $NO^\bullet$) and singlet oxygen ($[O_2(a^1\Delta_g)]$), all of which are important in biological reactions. From the interaction of the virus with these species emerges the disinfection power of the plasma, because it is thanks to these radicals and molecules that the virus is deactivated or degraded. The goal of an efficient CAP device is therefore to create a highly reactive environment while avoiding thermal effects that could cause degradation of the tissue along with the virus. What

will be then needed to study is which kind of radicals or molecules have the higher effect on the virus and what specifically happens to the virus, meaning at which level is the damage being done: degradation of the cellular capsid, damage to the DNA/RNA strand.
The plasma-virus interaction is addressed in every paper considered in this review; nonetheless, being this a physics thesis, the emphasis will be put on the physical and technological properties of the used plasma source, without dwelling into the specifics of the chemistry/biology involved.

1.5 Gas mixtures

The gas used to ignite the plasma can be ambient air, argon, helium and is frequently a mixture of the previous, such as argon with a percentage of ambient air or oxygen; frequently, a single study will consider different combinations of gases, to establish which one can grant the higher reactivity to the plasma. In fact, considering that the mechanism of disinfection is based on the interaction of the virus with reactive species, most studies focus on finding which species reacts more and is the primary responsible for virus deactivation and so the role of the feeding gas becomes central, because different mixtures produce different RS.

1.6 Lissajous figure method

By using an equivalent circuit model, it is possible to study the power dissipated in the plasma itself. In DBDs, the method of choice has become to measure the charge on the electrodes versus the applied voltage plot. DBDs with a single dielectric on one electrode can be represented by a series of two capacitances. One is the capacitance of the gap C_G, which depends on the dimensions and gas type, the other is the capacitance of the dielectric C_D. The total capacitance will then be $C_{tot} = C_G C_D/(C_G + C_D)$.

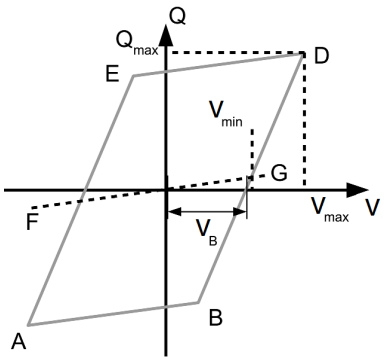

Figure 1.1: *Charge voltage curve for sinusoidally excited DBDs*

For calculations based on equivalent circuit models, the total capacitance needs to be measured. To do so, one can measure the current in time and determine the derivative of the time dependent voltage $V(t)$ (1.1) or measure the accumulated charge (1.1):

$$i(t) = C_{tot}\frac{dV(t)}{dt} \qquad \int_0^t i(t')dt' = Q(t) - Q(0) \tag{1.1}$$

and by integrating both sides of the first equation, one obtains:

$$C_{tot} = \frac{Q(t) - Q(0)}{V(t) - V(0)} \tag{1.2}$$

which equals the slope of line FG in Figure 1.1. The accumulated charge can be measured by introducing a capacitance in series with the electrodes and measuring the voltage drop across it. This capacitance C_M needs to be significantly larger than C_D and C_G. Measuring C_{tot} via (1.2) has the advantage of being less sensitive to noise compared to taking the derivative of the measured voltage according to (1.1). The enclosed area of the parallelogram measured in the charge-voltage diagram shown in Figure 1.1 yields the power per excitation cycle deposited into the dielectric barrier discharge. The discharge occurs at the paths BD and EA. No discharge is present at the paths DE and AB. The breakdown voltage V_B is the point where the Lissajous figure crosses the voltage axis. The area of the parallelogram (and thus the power per cycle) can be derived from

$$P_{cyc} = 4C_G V_0 \left(V_{max} - \frac{C_G}{C_{tot}}V_0\right) \tag{1.3}$$

The minimal required voltage for breakdown V_{min} is slightly higher than the actual gap voltage at breakdown V_B and depends on the capacitance of the system. Determining the maximum voltage V_{max} and charge Q_{max} for different applied voltages will result in a straight line in the Q–V plot of which the slope is C_D and it can be used even in short pulsed excited DBDs.

Chapter 2

Works that use DBD: a review

DBDs are the most frequently found kind of sources for what concerns virus deactivation; the vast majority of the articles considered in this thesis used a DBD to generate the plasma.
In 2008, Yasuda et al. [9] published an article regarding CAP sterilization, choosing to operate on wet samples of bacteria and bacteriophages, in the hope of finding more references to such research (at this point in time, research on virus deactivation was still new). Specifically, the goal was to find out more about the states of biological components on the way to cellular inactivation. In particular the bacteria-bacteriophage duo involved in this research was a *E.coli* and *bacteriophage* λ system.
The schematic of the device used can be seen in Figure 2.1, it consists of a stainless steel mesh (50

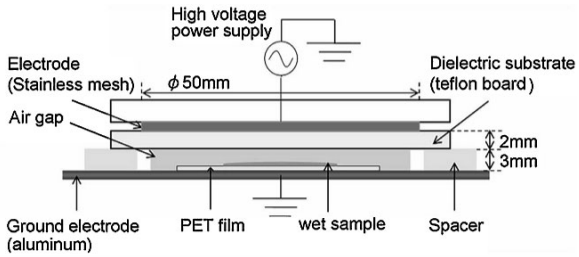

Figure 2.1: Schematic of the DBD for Yasuda

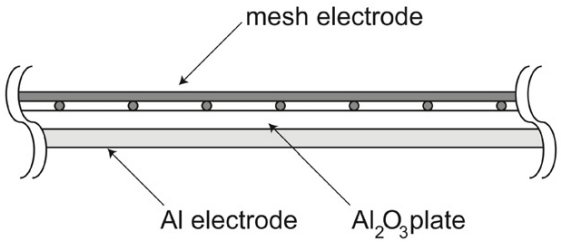

Figure 2.2: Schematic of the DBD for Zimmermann

mm ø, 20 mesh) used as high voltage electrode and an aluminium plate used as the ground one. The dielectric barrier was a Teflon sheet (2 mm thick), set on the high voltage electrode. In the atmospheric air gap (3 mm), an AC power unit (Kasuga-denki AGF-010) generated uniform filamentous streamers. All of the experiments in this article have been performed under fixed electrical conditions, except during operating time. The peak-to-peak voltage was of 40 kV p-p, the frequency of the applied voltage was 2 kHz and the input power was 8.8 W. The peak-to-peak voltage was adjusted using an oscilloscope and the input power was calculated using the Lissajous figure method from simple harmonic oscillations.
In this case, wet samples were used, meaning that the bacteria-bacteriophage duo was in solution when the DBD was applied. After DBD application of 5, 10, 20, 30, 40 s, samples were recovered and analyzed. Keeping the samples in a water solution has many experimental advantages, most importantly the efficiency of the bacterial inactivation is larger than using dried samples under the same electrical conditions [10]. The samples did not evaporate, meaning that there wasn't a significative rise in temperature, which remained low and harmless. Furthermore, it was noted that the solution's pH remained neutral even after 30 s of DBD treatment, but started to get acidic after 40 s, because of NO_x production.
Both *E.Coli* and λ-*phage* were successfully deactivated by DBD application, with λ-*phage* showing more rapid performance. Damage to the membrane, proteins and DNA were detected but not significantly, mainly appearing around 40 s of treatment, suggesting to be caused by the presence of acid in the solution. Finally, more than DNA damage or membrane destruction, it is the quick inactivation of proteins that may have a central role in sterilization by DBD.
In 2010, the same research team, still led by Yasuda, published another paper [11] in which they used

the same DBD device, focusing this time on all stages of phages deactivation, especially the beginning. They developed a method to evaluate in vivo damage of phage DNA and proteins separately. This time around, a different AC power source was used, specifically TREK Model 20/20C High Voltage Amplifier, equipped with a function generator (Agilent Function/Arbitrary Waveform Generator 33220A). The peak-to-peak voltage, frequency of the applied voltage, and input power were 40 kV p-p, 2 kHz and 8.7 W, respectively; the input power was again calculated using the Lissajous figure method. Again, wet state of samples was chosen.
The team focused on the first 20 s of discharge (5, 10, 20 s), because after this point acidification was found to be consistent; temperature of the samples did not exceed 40° even after 60 s of DBD application. Thanks to the new method developed to study damage of proteins and DNA separately, it was possible to conclude that protein damage occurs first and it is therefore responsible for virus deactivation; DNA damage increases with the increase of exposure time to plasma, still no synergetic effects with protein damage were observed.
In 2011, Zimmermann et al. [12], published one of the first works regarding plasma deactivation of actual viruses; they used a recombinant adenovirus (AdeGFPLuc) based on the replication defective human type 5 adenovirus. For what concerns the plasma device, Zimmermann used a cold atmospheric pressure plasma device, named FlatPlaSter, a common choice even among other authors [13] [14]. The device was similar to and inspired by the one used by Morfill et al. [15]. Specifically, it consisted of a SMD plasma electrode (10×10 cm^2) constructed as follows: the ground electrode was a mesh grid (stainless steel, 2.4 mesh cm^{-1}, wire diameter 0.5 mm), an insulator plate made of Al_2O_3 (1 mm thick) worked as a dielectric barrier and an aluminium plate (10 mm thick) constituted the high voltage electrode (Figure 2.2). The plasma is produced homogeneously on the mesh grid by applying an AC sinusoidal voltage 4.7 kV p-p at 10 kHz between the metal plate and the mesh grid. The power consumption of the electrode was 0.5 W cm^{-2}, evaluated with the Lissajous figure method using a 1 μF capacitor. The plasma is actually composed of many micro and nano discharges, one for each square of the mesh grid serving as ground electrode.
Treated adenoviruses in water solution were found to be deactivated by plasma treatment, especially by the interaction of ROS/RON species, identical to the ones our own immune system produces when reacting to a virus. No significant change of pH or increase in temperature has been observed, confirming that the responsible for deactivation it's plasma chemistry. A treatment of 240 s is sufficient to inhibit replication and to observe up to 6 log reduction.
In 2015 Ahlfeld et al [13] published another study based on a very similar device, the FlatPlaSter 2.0. Based on a surface microdischarge technology, it consists of a housing box designed to confine the plasma for laboratory tests. Inside, the SMD electrode has a three layer structure: a copper plate as the high voltage electrode, a stainless steel mesh (2.4 per cm, wire diameter of 0.5 mm) as the ground electrode and a 0.5 mm Teflon sheet in between as the dielectric material. The SMD electrode was mounted on the upper part of the housing box but it could also be used separately, by attaching the power source to it, as to freely move on the desired surface. To generate the plasma, a sinusoidal voltage from a Voltcraft 8202 function generator was amplified by a Trek amplifier and then applied to the HV electrode. The peak-to peak voltage and frequency were found to be 8.5 kV and 1 kHz, the power consumption of the plasma discharge was 30 mW/cm^2, always estimated using the Lissajous figure method. The plasma, which can be seen as a purple glow, was operated in ambient air and produced on the mesh electrode side.
The samples were constituted of NoV genotype GII.4, a kind of norovirus, and were dry. They were placed at a distance of 3 mm from the mesh surface, where the plasma was produced, and the tratment was conducted under ambient conditions, at 23.5 °C and 40% of relative humidity. Time of treatment varied amongst 0.5, 1, 2, 3, 4, 5, 10, or 15 min. The study concluded that CAPP treatment reduced the amount of a clinically relevant outbreak strain, NoV II.4, without any chemical residues; however, the initial viral load may influence the efficacy of CAPP treatment.
Also in 2015, Bae et al. [16] published a study regarding plasma deactivation of the murine norovirus (MNV-1), as a norovirus (NoV) surrogate and hepatitis A virus (HAV). The device used by Bae is referred to as plasma jet, a configuration commonly used in this field, and favoured by many other authors. A plasma jet is a DBD made of a cylindrical powered electrode with a sharpened tip, ending

with an emission hole, and a grounded electrode, usually positioned around the HV one; between them, dielectric material is placed, in contact with the HV electrode but not with the grounded one. The samples are positioned below the plasma jet and can be covered with some kind of container, made for example of glass. In this case, the emission hole had a diameter of 1.5 mm, around the HV electrode there was a dielectric and then the grounded electrode, which also had a cathode noozle as a cooling system; a glass container, covering the samples, was present. The schematic can be seen in Figure 2.3.

The plasma production parameters were a peak voltage of 3.5 kV and a frequency of 28.5 kHz; the

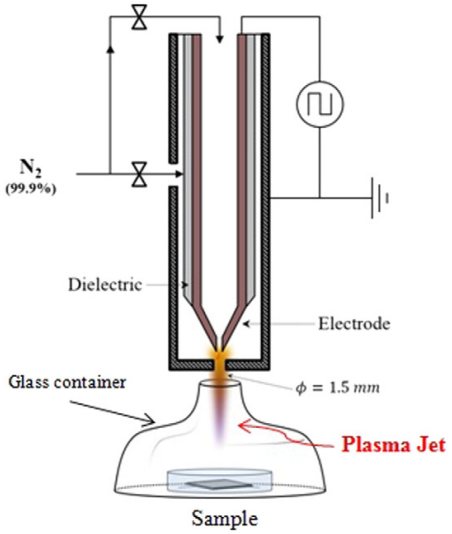

Figure 2.3: Schematic of the DBD for Bae

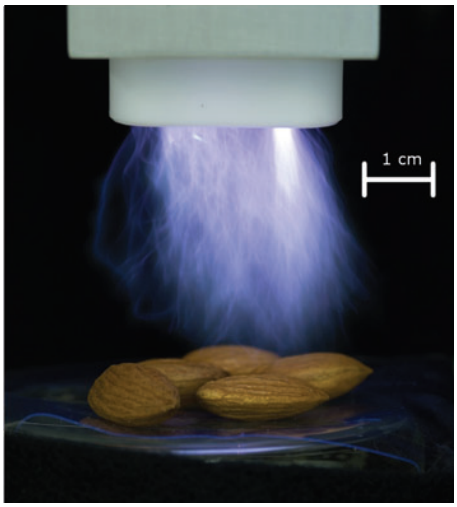

Figure 2.4: Plasma jet for Lacombe (Niemira)

discharge was ignited in nitrogen, with a N_2 (99.9%) flow rate at 6 standard liters per minute coming in the device. The distance between the jet nozzle and the surface of the sample was 4 cm. During treatment, samples were covered with a glass container and treated with APP in triplicates at 0.5, 1, 3, 5, 10, and 20 min. The results showed that all APP jet treatments decreased the levels of MNV-1 and HAV viruses; there was no effect on meat quality (the virus was inoculated in fresh meat) for treatment under 5 minutes.

Use of a plasma jet can be found also in a work by Lacombe et al. [17], who in 2015 studied deactivation of MNV-1, a surrogate for human norovirus, after being inoculated in blueberries, since their focus was on disinfecting food for mass distribution. The plasma device used in this study was previously described by Niemira et al. [18], who studied the effect of *Salmonella* and *E. coli* on whole almonds. The device used was a modified version of a Dyne-AMite HP (Enercon Corp.), based on a form of gliding arc plasma. Between the two shaped electrodes a 1 cm gap allows to establish a ionizing potential, which generates a plasma arc within a Teflon cowling. Thanks to the flow of feed gas at 4.13 atm the plasma arc is driven outward, expanded and cooled (Figure 2.4). The modification of the device from the original product consisted in allowing variation of electrical pulse frequency. On the basis of experiments by Niemira et al. [18] the plasma jet was adjusted to a pulse frequency of 47 kHz, with a power consumption of 549 W. The jars containing the samples (5 berries each) were positioned under the plasma jet at a distance of 7.5 cm, measured from the base of the Teflon cowling to the outside base of the jar. The jars were treated either with 0.11 m^3/min atmospheric CP alone for 0, 15, 30, 45, 60, 90, and 120 s, or with the CP jet and 0,2 m^3/min of ambient-temperature air, introduced via side nozzles. No thermal effect was found for treatment time <60 s, by introducing ambient air the samples were further cooled well below the level of thermal kill for norovirus surrogates, confirming the responsible for virus deactivation is once again plasma chemistry. The present study demonstrates a lab-scale CP system to inactivate viruses on the surface of blueberry in conjunction with force air cooling.

In 2015, Wu et al. [19] published an article regarding virus deactivation using different power levels and gas carriers. Aerosolized MS2 bacteriophage (ATCC 15597-B1) served as the challenge viral aerosol in this study. The APCP generator was previously described in a work by Liang et al. [20] in 2015;

a DBD system (Figure 2.5) made of a quartz tube (ø12 mm, 150 mm long), in which the discharge would take place, with a HV electrode, made of copper, and a ground electrode.

Wu tested the APCP generator with three different power levels, 20, 24, and 28 W, which correspond,

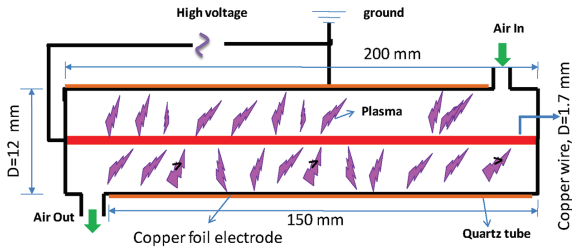

Figure 2.5: Schematic of the DBD for Wu

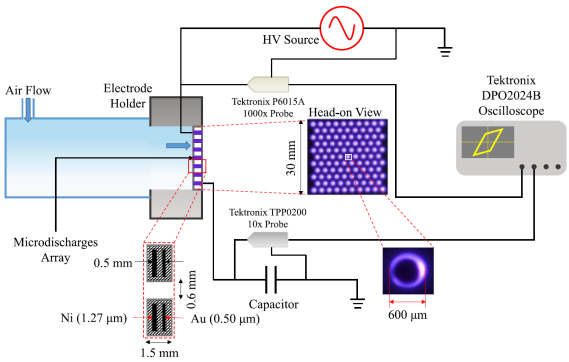

Figure 2.6: Schematic of the DBD for Nayak (2017)

respectively, to the three voltage and current sets: 30 V and 0.68 A, 30 V and 0.8 A, and 30 V and 0.93 A. Inside the tube, the viral aerosol was exposed to the APCP generated using three different gas carriers: ambient air, $He-O_2$ (2%, vol/vol), and $Ar-O_2$ (2%, vol/vol). On the basis of the dimensions of the plasma generation device and the exit flow rate, the exposure time for the virions inside the plasma device was calculated to be 0.12 s. Each of the viral aerosol samples was continuously collected for 20 min. The study concluded that inactivation of the MS2 viruses for both the airborne and waterborne states depends on the power level, exposure time, and gas carrier. Different gas carrier means different plasma chemistry, for example it has been found that optimizing the oxygen concentration in $He-O_2$ further enhances deactivation efficiency; in particular, Wu et al. considered a 3-min exposure to ACPC with $He-O_2$ (2%, vol/vol) but noted that selected oxygen percentage of between 0.5% and 1.5% in the $He-O_2$ gas carrier was reported to produce high levels of atomic oxygen, one of the reactive species responsible for deactivation [21]. In summary, RONS are still indicated as responsible for virus deactivation.

A study concerning a human virus that attacks the respiratory system was carried out in 2016 by Sakudo et al. [22], who studied the effect of plasma application on *adenovirus type 5*. The plasma device consisted of SI thyristor power supply (BLP-TES No.1), which generated short-time high-voltage pulses, two high voltage electrodes (anodes) and a ground electrode (catode) placed between them. The samples were put in a chamber box, which was filled with N_2 gas and maintained at a pressure of 0.5 atm during the electrical discharge at 1.5 kpps (kilo pulses per second).

The samples were subjected to treatment for 0 min (control), 5 min, 15 min at a temperature estimated around 45°C. The results indicate that oxidative stress induced by the presence of hydrogen peroxide appears to be the main mechanism of adenovirus inactivation. Additional factors may be involved: nitrogen gas related reactive chemical species such as nitrate and nitrite, intermediate molecular species generated during the formation of hydrogen peroxide, nitrate and nitrite may also contribute. Interestingly, NO and ROS are produced by immune systems for anti-microbial, immune modulation, cytotoxic, and cytoprotective roles [23]; findings from this study suggest that nitrogen gas plasma also elicits these effects.

Nayak et al. conducted two studies, featuring the same device, on feline calcivirus (FCV), one in 2017 [24] and one in 2019 [25]. For the 2017 study, the electrode arrangement (Figure 2.6) is more specifically described in [26]: it consists of an integrated coaxial microhollow discharge array electrode (Kyocera Inc.), made of two ultra thin metal electrodes, one gold one nickel, of unequal thickness, coated and separated by 500 μm thick layer of alumina (Al_2O_3). The gold electrode is thinner, grounded and located downstream of the gas flow; it's also the side where the emission is collected. The multilayered electrode consists of 105 through-holes, in which the discharge is created, arranged in a gridlike array and evenly distributed, with a diameter of 600 μm each. This electrode arrangement, constituting a coaxial-hollow discharge source, is then inserted in a holder made of polytetrafluoroethylene (PTFE), equipped with provision for HV electrical connections and attached to a polycarbonate

tube with a diameter of 45 mm in the upstream of the electrode. This tube allows air to flow through, making this plasma device a *flow-through* plasma reactor. An AC power source (PVM500) generates a sinusoidal HV signal at 20 kHz and applies it to the electrode at the opposite side of the detection and imaging diagnostics. The discharge power was estimated using the Lissajous figure method, through a capacitor (C=82 nF) with a capacitance much larger than that of the integrated coaxial microhollow discharge array ($\approx$ 70 pF).

For virus experiments, a platform with samples positioned on it was placed underneath the plasma source. The plasma setup could be moved vertically within a range of 2 mm–50 cm from the platform to obtain various exposure distances for the samples. The virus samples were either coated on stainless steel discs (gas-phase treatment) or suspended in an aqueous medium in wells of a 96-well microtiter plates (liquid-phase treatment). They were exposed to the reactive species produced by the array of microdischarges in the gas phase for a time ranging from 15 s to 10 min; the actual microdischarges, constituting the active plasma, were confined within the holes of the discharge geometry and so the samples were never in direct contact with the plasma. The aforementioned polycarbonate tube, attached to the downstream electrode, served to minimize the radial losses of plasma-generated reactive species to the surrounding air before they reached the virus samples.

The 2D array of micro-discharges was operated at atmospheric pressure in two gases: dry air (Laboratory Grade) and Ar + 20% O_2 (Ultra-Pure-Carrier Grade 99.9993%) at a constant total gas flow rate of 16.4 standard liters per minute (SLM). The discharge power for the air plasma was kept constant at 14.5 $\pm$ 0.3 W per cycle while for Ar + 20% O_2 plasma, it was adjusted to match the O_3 density in air (between 2.7 $\pm$ 0.1 and 16.1 $\pm$ 0.2 W per cycle). The power density was calculated by considering the combined area of all the micro holes rather than the whole area of the electrode, which was 30 times larger.

It was found that for gas-phase treatments humidifying the FCV-coated metal surface enhanced the virucidal activity, compared to the dry samples. The gas-phase treatment was also independent of the exposure distance. Comparing Ar + 20% O_2 plasma and air plasma, producing the same O_3 density, showed that both O_3 and RNS (NO_x) were responsible of the gas-phase FCV inactivation. In liquid-phase, however, RNS were the main responsible for viral inactivation; a correlation between pH drop, NO_2 concentration and virus inactivation was found and suggested that the inactivation occurs through acidified nitrites. It should be pointed out that different plasma reactors and flow systems can give rise to different chemical inactivation pathways. Plasma jets cause convection in the treated liquid causing enhanced mixing and species transfer from the gas to the liquid phase. A batch reactor typically does not have a convective flow and leads to the accumulation of NO_x that can cause ozone poisoning. The flow-through reactor studied in this work presents production of RNS and O_3 and both contribute to FCV inactivation.

In 2018 Guo et al [27] studied the effect of CAP on bacteriophages T4, Φ174, and MS2 and how water maintains the plasma's disinfecting properties after having been exposed to it. The DBD used in this work (Figure 2.7) was a surface discharge device, consisting of a plane HV electrode, a liquid-facing grounded mesh electrode, and a dielectric layer (made of polytetrafluoroethylene) between the two. Each mesh element has a hexagonal shape, and the plasma has good mesh-to-mesh homogeneity. A sinusoidal high voltage is applied and generates the plasma in the mesh elements of the ground electrode. The discharge power density was maintained at 0.2 W/cm^2.

The bacteriophage suspensions or water were placed underneath the plasma, the air gap between the plasma and the liquid surface was 8 mm. The surface air plasma and the bacteriophage suspension were sealed in a glass box. A gas mixture of argon and artificial air (79% N_2 plus 21% O_2) was flowed through the box at a constant rate of 4 liters/min, the volume ratio of artificial air was controlled at 1%. Compared to the surface discharge in air, the addition of argon enhanced the production efficiency of the reactive species and their fluxes underneath the bacteriophage suspension or water by diffusion. Plasma-activated water was studied and it was found that the inactivation of bacteriophages by plasma-activated water was efficient and time dependent. By storing PAW for 10 days, it was observed that it had lost some antiviral properties, probably due to decay of RONS, but that it was still efficient. There was no difference in plastic or glass storage and between keeping it away from light or exposed to it.

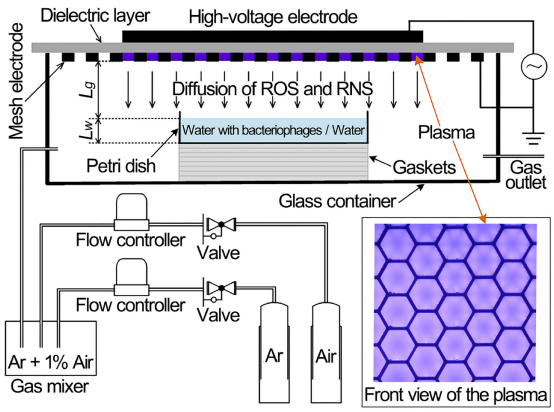

Figure 2.7: Schematic of the DBD for Guo

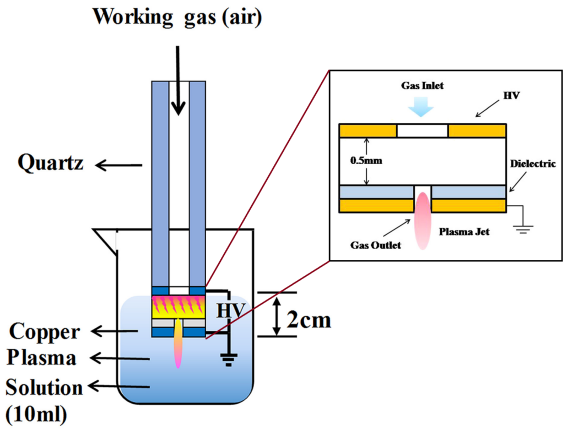

Figure 2.8: Schematic of the DBD for Su

The tratment times were 40, 80, 120 s for direct plasma treatment and 60, 120 s, 1h for PAW treatment. Plasma-based treatment efficiently inactivated different classes of viruses, with the primary responsible for inactivation being RONS.

Su et al. [3] performed a study on the deactivation of Newcastle Disease Viruse (NDV, LaSota strain) by plasma activated solutions (PAS). The solutions considered in this study were PAS(H_2O), PAS(NaCl), and PAS(H_2O_2), respectively obtained activating by plasma, for 10 min, 10-ml sterile distilled water, 0.9% NaCl, and 0.3% H_2O_2 solutions. PASs were so generated by plasma activation beneath the solution surfaces. The distance between the liquid surface and the plasma microjet (PMJ) end was 20 mm. The virus was injected in chicken embryos and after 24 hours allantoic fluids were harvested and treated with PAS(H_2O), PAS(NaCl) and PAS(H_2O_2) at ratios of 1:3, 1:5, and 1:9, respectively, for 30 min. This study concluded that a PAS has the potential to inactivate NDV. PAS(H_2O), PAS(NaCl) and PAS(H_2O_2) can completely inactivate NDV at an appropriate ratio, verified by ELA and HA tests.

The plasma device used was described by Yu et al. [28]; it consisted in a DBD with hollow electrodes (HEDBS) as presented in Figure 2.8. The high voltage and ground electrode were both made of copper, a quartz plate attached to the inner surface of the ground electrode served as dielectric. On the centre of the HV and the ground electrode, respectively, were positioned the gas inlet (ø1.5 mm) and outlet (ø0.5 mm). The whole device was 5 mm long. The HEBDS was excited by AC current at a frequency of 20 kHz and with a peak voltage of 25 kV. Homogeneous plasma was produced in the discharge gap of 0.5 mm and was ejected through the outlet, reaching 7 mm long. Tracing a map of the electric field distribution, allows to conclude that there is no electric field intensity outside the HEDBS, making it safe from common shock hazard from strong electric field.

The working gas was air with a 4.3 l/min (or 260 liter/hour) flow rate and it was injected into the quartz tube. Differences in electron density when varying the flow rate were also studied: the electron density will increase with the decrease in outlet diameter from 1.5 mm to 0.5 mm when flow rate is fixed at 5 l/min (Fig. 2.9). Considering flow rates of 3.5 l/min, 5 l/min, and 6.5 l/min and outlet diameter fixed at 0.5 mm, the larger the flow rate, the higher the electron density, as shown in Figure 2.10. When the air flow rate reaches 6.5 l/min, the electron density is $5.29 \cdot 10^{15}$ cm^{-3}. The same trend was observed both in the discharge current and electron temperature.

From fluidodinamic considerations made in the article, it can be concluded that the HEDBS had a remarkable recoil effect on the discharge gas flow, which could increase discharge gas pressure inside. Considering the Townsend mechanism of electric breakdown of gases, electric breakdown starts with the electron avalanche, which is the multiplication of primary electrons through cascade ionization. When the air flow rate is increased or the outlet diminished, gas pressure becomes larger, and so more gas molecules will be excited in discharge. The temperature of particles inside also increases. Both the electron-impact ionization rate coefficient and ionization cross section will be enlarged with the increased electron temperature. However, when the temperature rises, the radiative recombination rate coefficient will descend, and so fewer electrons will participate in the recombination reaction. To

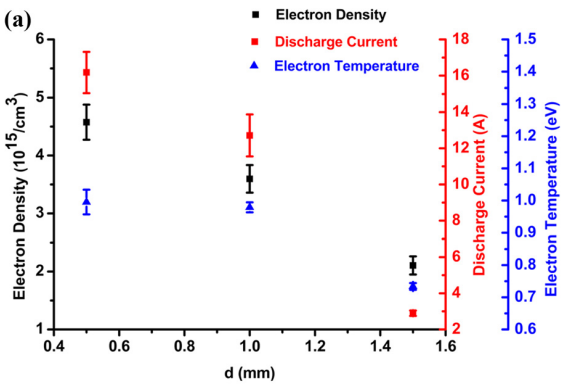

Figure 2.9: Electron density, discharge current, electron temperature vs distance

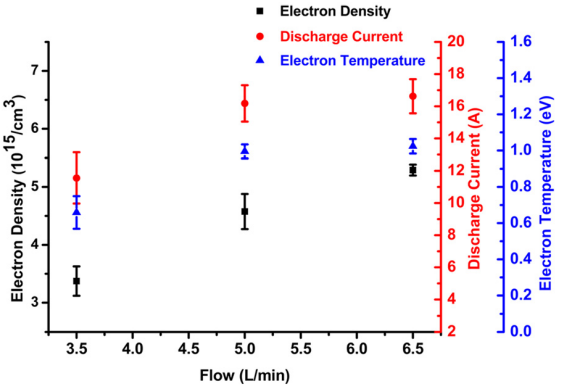

Figure 2.10: Electron density, discharge current, electron temperature vs flow

summarize, the increase in pressure together with particle temperature, including electron temperature, achieves that electron density will be enhanced as well as more reactive species will be generated with a high efficiency.
In a study by Xia et al. [29], in 2019, viral aerosols of Bacteriophage MS2 (ATCC 15597-B1) in an airstream were subjected to CAP exposure for 30, 60 min. The study concluded that aerosolized MS2 was predominantly inactivated by radicals and other reactive oxygen species (ROS) generated by the packed-bed NTP reactor over the short exposure time and that ozone acted as a secondary inactivating reagent.
In this article a packed-bed NTP in-flight airstream disinfection process was studied, in particular consisting of a DBD non thermal plasma reactor, responsible of treating the viral aerosols. Such reactor, described in Figure 2.11, is composed of a Plexiglas tube (OD 10.2 cm; ID 9.5 cm; length 20.3 cm) and two smaller tubes (OD 8.9 cm; ID 7.6 cm; length 30.5 cm). The smaller tubes can slide freely relatively to the larger tube due to a clearance of 0.3 cm. Two rubber O-rings, sitting in the grooves on the OD of the smaller tube, permit an air-tight sliding mechanism. A circular perforated brass plate, installed at the end of each sliding tube, serves as the ground electrode and evenly distributes the inlet and outlet flow of the reactor. The sliding electrode allows for depth adjustment between 0.6

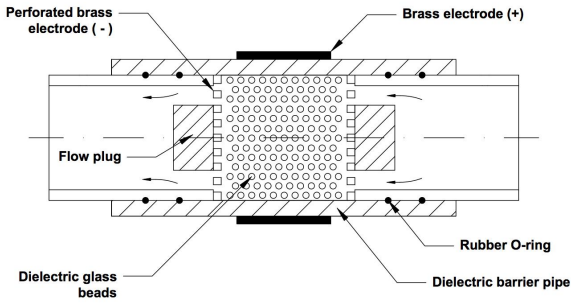

Figure 2.11: Schematic of the DBD for Xia

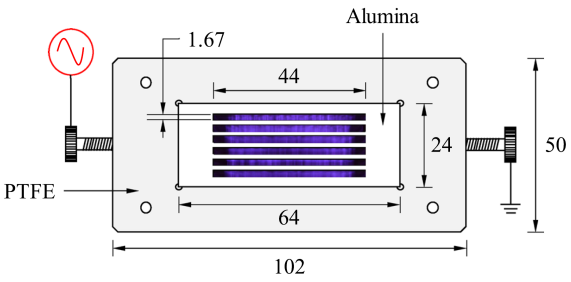

Figure 2.12: Schematic of the DBD for Nayak

and 12.7 cm. Two flow spines made of styrofoam (OD 6.35 cm) are put at the center of the reactor to direct the airflow with the viral aerosols through an annular region where the plasma is concentrated. A brass ring (thickness 0.9 mm, width 2.5 cm) attached to the OD of the larger Plexiglas tube serves as the HV electrode for the AC high voltage supply. The DBD reactor can be powered by two different AC voltage amplifiers: a variable 0 to 20 kV (peak-to-peak) high voltage amplifier and a 30 kV neon transformer. The first is coupled with a digital function generator, which outputs 60 Hz sinusoidal AC voltage. The amplifier can output applied voltage signals (V) at 1 V/1000 V and two current signals (I), total current and return current, at 1 V/200 μA. For the 30 kV neon transformer, a high voltage probe (1 V/1000 V) and a Pearson current coil (1V/1A) are connected to one of the power supply's high voltage electrodes. The microdischarge is generated through a dielectric barrier made of Plexiglas. The packed-bed, consisting of 500 inert borosilicate glass beads (ø0.6 cm), serves to enhance

the microdischarge by partial discharges at the contact points between the glass beads, for effective electron-viral aerosol collisions and inactivation process.
In 2019, Nayak et al [25], published another study regarding a flow-through volumetric DBD reactor, which can be seen in Fig. 2.12. The DBD reactor is made of seven thin metallic plate electrodes (HV and grounded) in an alternating pattern, each separated and covered by alumina as the dielectric material. As a result, there are six rectangular slits corresponding to the active discharge zones. The electrode arrangement is encased in a holder made of polytetrafluoroethylene (PTFE), with provision for high voltage and ground electrical connections. This reactor is then mounted inside the test section of a wind tunnel and sealed using a rubber gasket to prevent infiltration of untreated air.
The discharge is ignited in the rectangular slits by a high-voltage sinusoidal signal with a frequency in the 26–29 kHz range, which is generated by an AC power source. The signal is modulated at a 1 kHz modulation frequency with a duty cycle of 12.5%, 25%, or 50% using a function generator. This modulation allows to operate the discharge at different average power levels for fixed instantaneous plasma power. Applied voltage ranges from 12.9 to 14.9 kV. The applied voltage (V) was measured using a HV probe, and the charge (Q) was obtained by measuring the voltage (V_C) across a capacitor (C = 100 nF) in series with the plasma reactor. The corresponding waveforms were recorded by a digital oscilloscope. The power (P) dissipated in the discharge is calculated from the Lissajous plots.
In this study PRRS virus (strain VR2332) was used, after being propagated in monkey kidney cells. The areosolized virus would flow through the wind tunnel for 5 or 10 minutes of sampling, after which the device would be shut down and samples collected.
The study concluded that the volumetric DBD was effective at inactivating aerosolized PRRS virus in a wind tunnel within a few milliseconds; furthermore, the inactivation effect was independent of the discharge power and the sampling time. O_3 and H_2O_2 do not play a direct role in the inactivation while ONOOH could initiate specific pathways to have a virucidal effect in the effluent of the discharge. Most likely, virus inactivation during in situ droplet treatment is further enhanced by short-lived species such as, $^{\bullet}OH$ and $O_2(a^1\Delta_g)$.

Chapter 3

Works that use RF and UV: a review

Of all the articles considered, the only ones using a RF generated plasma to deactivate viruses were all published by the same author, Aboubakr et al [30] [31] [32]. In three different papers the team of researchers studied different aspects of the same plasma device, schematised in Figure 3.1. Structurally, it was a plasma jet: a plastic enclosure contains a concentric powered needle electrode (ø1 mm) surrounded by a glass tube (ø1.65 mm) and a 5 mm long ground ring electrode, positioned at the end of the glass tube. The plasma is ignited in Ar, which is blown through a 1.9 mm quartz tube at 1.5 liters/min by RF power at 13.56 MHz.

The RF power is modulated at a frequency of 20 kHz with a duty cycle of 20% and the work was performed at a time-averaged plasma dissipated power of 2.5 W. A detailed explanation of how the power level was measured can be found at [33].
4 different gases were used: Ar, Ar plus 1% O_2, Ar plus 1% dry air, and Ar plus 0.27% water. The amounts of admixtures were controlled by mass flow controllers. For Ar plus 0.27% water, part of the Ar flow was sent through a bubbler with distilled water in order to humidify the Ar gas. A sterile 96-well microtiter plate containing virus in suspension, which in this case was FCV, was put below the plasma jet as to allow the tip of the plasma plume to approach the top of the well. The samples were exposed to plasma generated at five power levels (1±0.1, 1.5±0.1, 2±0.1, 2.5±0.1, 3±0.1 W). The distance between the surface of the treated viral suspension and the plume was 18.13 mm. The exposure times were 0 (control), 15, 30, 60, 120, and 180 s. Different distances between plume and virus suspension were considered and it was seen that by changing gas admixtures would change the length of the plasma plume, rating them from longest to shortest: Ar, Ar plus 1% air, Ar plus 0.27% water, Ar plus 1% O_2.

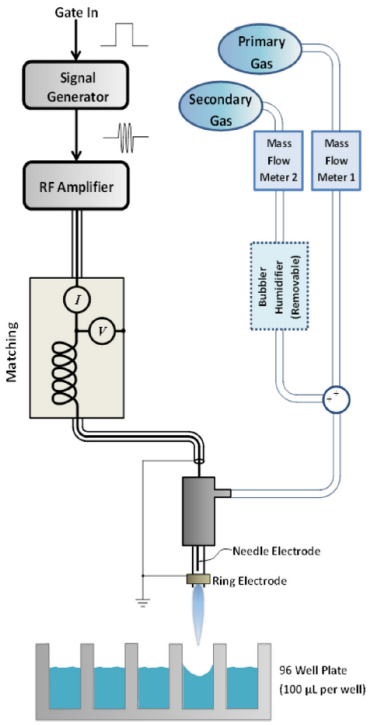

Figure 3.1: APPJ for Aboubakr

The study concluded that reduction in the virus titer increased with increasing exposure time and decreasing exposure distance. The highest virucidal effect was obtained with Ar plus 1% O_2 plasma and the lowest with Ar plus 0.27% water plasma. Changes in temperature and pH and formation of H_2O_2 were noted but not responsible for the virucidal effect of plasma. Once again, the effects of reactive oxygen and nitrogen species were thought to be responsible for the virucidal effect.

UV plasma

The case of a UV generated plasma was found to be a single case amongst the consulted articles. In 2009, Terrier et al. [34], studied the deactivation of airborne respiratory viruses with cold oxygen plasma. In particular, RSV, hPIV-3 and A (H5N2) influenza viruses were considered.

The employed device was developed by Biozone scientific firm and it worked by subjecting air by high energy deep-UV light with an effective radiation spectrum between 180 nm and 270 nm. The resulting cold gas plasma is composed of several species: negative and positive ions, free radical molecules, electron, UV-photons and ozone. The paper concludes that this method of disinfection is indeed effective for all three of the considered viruses.

In the article, nothing was said about the precise structure of the COP device and nothing could be found on the Biozone company website (`http://biozonescientific.com/`). Furthermore, it is not clear how the COP device works, since from the UV length they affirm to use, one could only obtain photons with an energy of ≈ 6.8 eV, which is insufficient to ionize both oxygen and nitrogen, preventing the electron avalanche, at the origin of the discharge that generates the plasma, from taking place.

Power dissipation in RF plasmas

Measuring dissipated power in RF plasmas is more difficult than for DBDs. The average power in an electrical discharge is calculated by:

$$P = f \int_0^{1/f} I(t)V(t)dt \tag{3.1}$$

where $I(t)$ and $V(t)$ are the current and voltage signals, f is the frequency of the electric excitation. For a sinusoidal excitation, the power can be calculated from the mean values of voltage ($V_{RMS} = V/\sqrt{2}$) and current ($I_{RMS} = I/\sqrt{2}$) signals and their phase difference ϕ:

$$P = I_{RMS} V_{RMS} \cos\phi \tag{3.2}$$

In RF discharges, however, when using voltage probes for the voltage measurements, the probe's capacitance has a strong influence on the resonance matching circuit of the RF setup, since the reactance and resistance of the voltage probe are tipically in the same order of magnitude as the ones for the matching unit and plasma source. Furthermore, the phase ϕ results in large measurement errors, as an estimation by error propagation reveals. An off-resonance phase-difference of 89°, and a measurement error of 1% in voltage, current, and phase, will result in an error in the power measurement of almost 90%. [7]

One way to determine voltage and current in an RF discharge is to use a full equivalent circuit model of the plasma source and the measuring probe. A simpler approach is to use a basic matching unit consisting only of a coil. Measuring current and voltage between the power amplifier and the matching unit, instead of after the matching unit allows to operate the plasma at impedance matched conditions without the influence of the probes. The power dissipated in the plasma can then be calculated from differences of the root mean square values of the power dissipated in the system with the plasma switched off and the dissipated power with the plasma switched on. This works, assuming that the power consumed within the matching coil is constant, independent of the state of the plasma source. It's also necessary to take into consideration that in RF discharges, especially above 13.56 MHz, the RF wavelengths lie in the meter range, within the dimensions of the used cables. This means that positioning of the probes has an influence on the measurement due to local minima or maxima of the wave. Also, a distinction between forward and backward propagating signal needs to be made. Instead of voltage and current probes, directional couplers can be used. A calibration will provide the coupling factors for the forward directed signal (k_F) and the backward directed one (k_B). The dissipated power (with plasma switched on and plasma switched off) can then be calculated from the forward voltage V_F and the backward voltage V_B:

$$P_{off/on} = \frac{V_{F,\ off/on}^2 k_F^2 - V_{B,\ off/on}^2 k_B^2}{50\ \Omega} \tag{3.3}$$

Error propagation on 3.3 with the same error estimation of 1% used for 3.2 yields a maximum error of 10%. [7]

Summary table

Authors	Source	Gas used	Virus	Treatment time
Yasuda et al. [9]	DBD	ambient air	*λ-phage*	5,10,20, 30,40 s
Yasuda et al. [11]	DBD	ambient air	*λ-phage*	5,10,20 s
Zimmermann et al. [12]	DBD	ambient air	AdeGFPLuc	240 s
Ahlfeld et al. [13]	DBD	ambient air	NoV GII.4	0.5,1,2,3,4, 5,10,15 min
Bae et al. [16]	DBD	ambient air	MNV-1, HAV	0.5,1,3,5 10,20 min
Lacombe et al. [17]	DBD	ambient air	MNV-1	0,15,30,45 60,90,120 s
Wu et al. [19]	DBD	ambient air $He-O_2$ (2%, vol/vol) $Ar-O_2$ (2%, vol/vol)	MS2	30,60,120,180 s
Sakudo et al. [22]	DBD	N_2 gas	Adenovirus type 5	0,5,15 min
Nayak et al. [24]	DBD	dry air Ar + 20% O_2	FCV	[15 s;10 min]
Guo et al. [27]	DBD	79% N_2 + 21% O_2	Φ174, and MS2	40,80,120 s 60,120 s,1 h
Su et al. [3]	DBD	ambient air		30 min
Nayak et al. [25]	DBD	ambient air	PRRS	5,10 min
Xia et al. [29]	DBD	ambient air	MS2	30,60 min
Aboubakr et al. [30]	RF	Ar Ar plus 1% O_2 Ar plus 1% dry air Ar plus 0.27% water	FCV	0,15,30, 60,120 s
Aboubakr et al. [31]	RF	Ar Ar plus 1% O_2 Ar plus 1% dry air Ar plus 0.27% water	FCV	0,15,30, 60,120 s
Aboubakr et al. [32]	RF	99% argon-1% O_2	FCV	15 s, 2 min
Terrier et al. [34]	UV	ambient air	RSV hPIV-3 A (H5N2)	3 min

Table 3.1: Summary of the articles quoted in this thesis

Conclusions

In this work the existing literature on virus deactivation by cold plasma application was reviewed, divided by the type of plasma source used to generate the plasma. It can easily be seen that the vast majority of the articles used a DBD to perform their experiments, while only one author used a RF generated plasma for virus deactivation. An UV kind of source represented a single case, not even well detailed from the physics perspective. It can then be concluded that, at the moment, the preferred source for this kind of study is the DBD. Furthermore, many of the DBDs studied in this thesis presented themselves in the form of plasma jets.
What can also be concluded is that the current literature is quite limited, especially if compared to the one about bacteria and fungi deactivation. However, it can be expected, given the current situation with the COVID-19 pandemic, that more and more research teams will focus on virus deactivation by cold plasma application, since the results achieved in the articles reviewed appear to be highly promising.

Bibliography

[1] G. Isbary *et al.*, "Randomized placebo-controlled clinical trial showed cold atmospheric argon plasma relieved acute pain and accelerated healing in herpes zoster," *Clinical Plasma Medicine*, vol. 2, pp. 50–55, dec 2014.

[2] O. Alekseev *et al.*, "Nonthermal dielectric barrier discharge (DBD) plasma suppresses herpes simplex virus type 1 (HSV-1) replication in corneal epithelium," *Translational Vision Science & Technology*, vol. 3, p. 2, mar 2014.

[3] X. Su *et al.*, "Inactivation efficacy of nonthermal plasma-activated solutions against newcastle disease virus," *Applied and Environmental Microbiology*, vol. 84, feb 2018.

[4] S. Kanazawa *et al.*, "Stable glow at atmosphericpressure," *J. Phys. D Appl. Phys. 21 838–840*, 1988.

[5] F. Massines *et al.*, "Experimental study of an atmospheric pressure glow discharge application to polymers surface treatment," *Proceedings of the GD-92, Swansea, UK, Vol. 2, pp. 730–733*, 1992.

[6] J. Roth *et al.*, "Experimental generation of a steady-stateglow discharge at atmospheric pressure," *Proc. IEEE Int. Conf. Plasma Sci.*, p. 170–171, 1992.

[7] X. Lu *et al.*, *Nonequilibrium Atmospheric Pressure Plasma Jets: Fundamentals, Diagnostics, and Medical Applications*. CRC Press, 2019.

[8] M. Laroussi, M. G. Kong, G. Morfill, and W. Stolz, *Plasma Medicine: Applications of Low-Temperature Gas Plasmas in Medicine and Biology*. Cambridge University Press, 2012.

[9] H. Yasuda *et al.*, "States of biological components in bacteria and bacteriophages during inactivation by atmospheric dielectric barrier discharges," *Plasma Processes and Polymers*, vol. 5, pp. 615–621, aug 2008.

[10] M. Tanino *et al.*, "Sterilization using dielectric barrier discharge at atmospheric pressure," *Int. J.Plasma Environ. Sci. Technol.*, vol. 1, p. 102, 2007.

[11] H. Yasuda *et al.*, "Biological evaluation of DNA damage in bacteriophages inactivated by atmospheric pressure cold plasma," *Plasma Processes and Polymers*, vol. 7, pp. 301–308, mar 2010.

[12] J. L. Zimmermann *et al.*, "Effects of cold atmospheric plasmas on adenoviruses in solution," *Journal of Physics D: Applied Physics*, vol. 44, p. 505201, nov 2011.

[13] B. Ahlfeld *et al.*, "Inactivation of a foodborne norovirus outbreak strain with nonthermal atmospheric pressure plasma," *mBio*, vol. 6, jan 2015.

[14] T. Maisch *et al.*, "Decolonisation of MRSA, s. aureus and e. coli by cold-atmospheric plasma using a porcine skin model in vitro," *PLoS ONE*, vol. 7, p. e34610, apr 2012.

[15] G. E. Morfill *et al.*, "Nosocomial infections—a new approach towards preventive medicine using plasmas," *New Journal of Physics*, vol. 11, p. 115019, nov 2009.

[16] S.-C. Bae *et al.*, "Inactivation of murine norovirus-1 and hepatitis a virus on fresh meats by atmospheric pressure plasma jets," *Food Research International*, vol. 76, pp. 342–347, oct 2015.

[17] A. Lacombe *et al.*, "Nonthermal inactivation of norovirus surrogates on blueberries using atmospheric cold plasma," *Food Microbiology*, vol. 63, pp. 1–5, may 2017.

[18] B. A. Niemira, "Cold plasma reduction of salmonella and escherichia coli o157:h7 on almonds using ambient pressure gases," *Journal of Food Science*, vol. 77, pp. M171–M175, mar 2012.

[19] Y. Wu *et al.*, "MS2 virus inactivation by atmospheric-pressure cold plasma using different gas carriers and power levels," *Appl. and Env. Microbiology*, vol. 81, pp. 996–1002, nov 2014.

[20] Y. Liang *et al.*, "Rapid inactivation of biological species in the air using atmospheric pressure nonthermal plasma," *Environmental Science & Technology*, vol. 46, pp. 3360–3368, mar 2012.

[21] S. Wang *et al.*, "Oxygen effects on a He/O_2 plasma jet at atmospheric pressure," *IEEE Transactions on Plasma Science*, vol. 37, pp. 551–554, apr 2009.

[22] A. Sakudo *et al.*, "Nitrogen gas plasma generated by a static induction thyristor as a pulsed power supply inactivates adenovirus," *PLOS ONE*, vol. 11, p. e0157922, jun 2016.

[23] A. V. Belikov *et al.*, "T cells and reactive oxygen species," *Journal of Biomedical Science*, vol. 22, oct 2015.

[24] G. Nayak *et al.*, "Reactive species responsible for the inactivation of feline calicivirus by a two-dimensional array of integrated coaxial microhollow dielectric barrier discharges in air," *Plasma Processes and Polymers*, vol. 15, p. 1700119, sep 2017.

[25] G. Nayak *et al.*, "Rapid inactivation of airborne porcine reproductive and respiratory syndrome virus using an atmospheric pressure air plasma," *Plasma Processes and Polymers*, feb 2020.

[26] G. Nayak *et al.*, "Effect of air flow on the micro-discharge dynamics in an array of integrated coaxial microhollow dielectric barrier discharges," *Plasma Sources Science and Technology*, vol. 26, p. 035001, feb 2017.

[27] L. Guo *et al.*, "Mechanism of virus inactivation by cold atmospheric-pressure plasma and plasma-activated water," *Applied and Environmental Microbiology*, vol. 84, jun 2018.

[28] S. Yu, Q. Chen, J. Liu, K. Wang, Z. Jiang, Z. Sun, J. Zhang, and J. Fang, "Dielectric barrier structure with hollow electrodes and its recoil effect," *Applied Physics Letters*, vol. 106, p. 244101, jun 2015.

[29] T. Xia *et al.*, "Inactivation of airborne viruses using a packed bed non-thermal plasma reactor," *Journal of Physics D: Applied Physics*, vol. 52, p. 255201, apr 2019.

[30] H. A. Aboubakr *et al.*, "Virucidal effect of cold atmospheric gaseous plasma on feline calicivirus, a surrogate for human norovirus," *Applied and Environmental Microbiology*, vol. 81, pp. 3612–3622, mar 2015.

[31] H. A. Aboubakr *et al.*, "Inactivation of virus in solution by cold atmospheric pressure plasma: identification of chemical inactivation pathways," *Journal of Physics D: Applied Physics*, vol. 49, p. 204001, apr 2016.

[32] H. A. Aboubakr *et al.*, "Cold argon-oxygen plasma species oxidize and disintegrate capsid protein of feline calicivirus," *PLOS ONE*, vol. 13, p. e0194618, mar 2018.

[33] S. Hofmann *et al.*, "Power dissipation, gas temperatures and electron densities of cold atmospheric pressure helium and argon RF plasma jets," *Plasma Sources Science and Technology*, vol. 20, p. 065010, nov 2011.

[34] O. Terrier *et al.*, "Cold oxygen plasma technology efficiency against different airborne respiratory viruses," *Journal of Clinical Virology*, vol. 45, pp. 119–124, jun 2009.